Quantification of Striatal Dopamine Transporters with ^{123}I-FP-CIT SPECT Is Influenced by the Selective Serotonin Reuptake Inhibitor Paroxetine: A Double-Blind, Placebo-Controlled, Crossover Study in Healthy Control Subjects

Jan Booij[1,2], Jan de Jong[1], Kora de Bruin[1], Remco Knol[1,2], Maartje M.L. de Win[2,3], and Berthe L.F. van Eck-Smit[1]

[1]Department of Nuclear Medicine, University of Amsterdam, Academic Medical Center, Amsterdam, The Netherlands; [2]Graduate School for Neurosciences, Amsterdam, The Netherlands; and [3]Department of Radiology, University of Amsterdam, Academic Medical Center, Amsterdam, The Netherlands

Dopamine transporter (DAT) imaging with ^{123}I-FP-CIT (^{123}I-*N*-ω-fluoropropyl-2β-carbomethoxy-3β-(4-iodophenyl)nortropane) SPECT is frequently used to detect loss of nigrostriatal cells in parkinsonism. Recent ^{123}I-β-CIT (^{123}I-2β-carbomethoxy-3β-(4-iodophenyl)tropane) studies have shown a significant increase in striatal-to-nonspecific β-CIT binding ratios after treatment with selective serotonin reuptake inhibitors (SSRIs). Due to similarities between ^{123}I-β-CIT and ^{123}I-FP-CIT (both are derived from cocaine and show relatively high affinity for the DAT and the serotonin transporter [SERT]), we hypothesized that quantification of striatal ^{123}I-FP-CIT binding may be influenced by SSRIs. Moreover, we hypothesized that ^{123}I-FP-CIT in humans binds not only to DATs but also to central and peripheral SERTs. **Methods:** To study the influence of the SSRI paroxetine on ^{123}I-FP-CIT binding to DATs in the striatum, we conducted a double-blind, placebo-controlled, crossover study with paroxetine in 8 healthy young male control subjects. In addition, we studied whether paroxetine was able to block ^{123}I-FP-CIT binding in SERT-rich brain areas and in lung tissue, as lung tissue contains a considerable amount of SERTs. Participants were pretreated for 2 d with paroxetine (20 mg/d) or placebo at 2 sessions (crossover design), and brain SPECT was performed 1 and 3 h after ^{123}I-FP-CIT injection, whereas lung uptake was measured 2 h after injection. **Results:** Compared with placebo pretreatment, we found after paroxetine pretreatment a statistically significant increase (approximately 10%) in specific striatal-to-nonspecific ^{123}I-FP-CIT binding ratios at 3 h after injection, a time point at which striatal ^{123}I-FP-CIT binding ratios are stable. In addition, after paroxetine treatment, statistically significantly lower binding ratios were found in SERT-rich brain areas (e.g., at 1 h after injection, midbrain-to-cerebellar ratios were approximately 90% lower) as well as significantly lower uptake in lung tissue was found (approximately 40% lower after paroxetine). **Conclusion:** In this study we show that the quantification of striatal ^{123}I-FP-CIT binding to DAT is significantly increased by the SSRI paroxetine in humans. To our knowledge, this is the first study which shows that ^{123}I-FP-CIT binds in vivo in humans not only to DATs but also to central SERTs and SERTs in lung tissue.

Key Words: FP-CIT SPECT; dopamine transporter; serotonin transporter; paroxetine

J Nucl Med 2007; 48:359–366

The dopamine transporter (DAT) is expressed exclusively on the terminal of dopaminergic neurons, with the highest expression in extrasynaptic plasma membranes (*1*). The SPECT tracer ^{123}I-FP-CIT (^{123}I-*N*-ω-fluoropropyl-2β-carbomethoxy-3β-(4-iodophenyl)nortropane) labels this transporter in vivo (*2*). Since 1996, many studies from different centers have shown consistently that ^{123}I-FP-CIT SPECT is a sensitive means to detect dopaminergic degeneration in Parkinson's disease (PD), even at the earliest clinical motor stages, and it may possibly also play a role in detecting dopaminergic degeneration at the preclinical phase of PD (*3–7*). Moreover, several studies have shown that ^{123}I-FP-CIT SPECT could be used to detect dopaminergic degeneration in neurologic diseases other than PD but characterized by dopaminergic degeneration (*6,8*). On the other hand, in diseases without evidence of dopaminergic degeneration, but commonly misdiagnosed as parkinsonism (e.g., essential tremor or drug-induced parkinsonism), ^{123}I-FP-CIT SPECT images were graded as normal (*9,10*). Because of its well-validated ability to detect degeneration of nigrostriatal dopaminergic neurons in vivo, ^{123}I-FP-CIT has been registered in Europe as DaTSCAN (GE Healthcare) since 2000.

After its registration, the use of ^{123}I-FP-CIT SPECT for routine clinical as well as scientific studies has increased dramatically, particularly in Europe. Although it has been

Received Sep. 26, 2006; revision accepted Nov. 20, 2006.

For correspondence or reprints contact: Jan Booij, MD, Department of Nuclear Medicine, F2N, University of Amsterdam, Academic Medical Center, Meibergdreef 9, 1105 AZ Amsterdam The Netherlands.

E-mail: J.Booij@amc.uva.nl

COPYRIGHT © 2007 by the Society of Nuclear Medicine, Inc.

validated that visual assessment of ^{123}I-FP-CIT SPECT images is a sensitive tool to detect degeneration in clinical studies (*9*), many centers also use quantification techniques (e.g., region-of-interest [ROI] methods) for such studies (*3–7,9,11*).

Recently, several studies have shown that the quantification of striatal $^{123/125}$I-β-CIT binding ratios may be influenced by selective serotonin reuptake inhibitors (SSRIs), although the exact mechanism is not entirely understood (*12–15*). Like ^{123}I-β-CIT (2β-carbomethoxy-3β-(4-iodophenyl)tropane), ^{123}I-FP-CIT is derived from cocaine and is a nonselective radiotracer for the DAT (*15,16*). Whereas β-CIT (RTI-55) has a high affinity for both DATs and serotonin transporters (SERTs), the affinity of FP-CIT (RTI-313) for SERTs is also relatively high, although it is more selective for DATs (50% inhibitory concentration [IC_{50}] for DAT and SERT, 1.67 and 16.3 nmol/L, respectively (*17*)). Because of the similarities between ^{123}I-β-CIT and ^{123}I-FP-CIT, it could be hypothesized that also the quantification of striatal ^{123}I-FP-CIT binding to DATs may be influenced by SSRIs. Although ^{123}I-FP-CIT is used frequently, this hypothesis has not been tested. Evaluation of this hypothesis is relevant because the prevalence of depression in PD is high, and SSRIs are the most commonly prescribed antidepressants in this group of patients (*18*). Therefore, we used a double-blind, placebo-controlled, crossover design with the SSRI paroxetine to study the possible influence of paroxetine on ^{123}I-FP-CIT binding to DATs in the DAT-rich striatum. Moreover, we studied whether paroxetine was able to block ^{123}I-FP-CIT binding in SERT-rich brain areas, and in lung tissue (also rich in SERTs (*19*)), as previous β-CIT studies suggested that blockage of peripheral SERTs may play a role in the increased striatal binding after the use of SSRIs (*15*). As paroxetine selectively blocks SERTs, and taking into account recent findings with ^{123}I-β-CIT SPECT (*12–14*), we hypothesized that paroxetine would cause a significant increase in specific striatal-to-nonspecific ^{123}I-FP-CIT binding ratios. Finally, we hypothesized that paroxetine would significantly block ^{123}I-FP-CIT binding to central as well as peripheral SERTs.

MATERIALS AND METHODS

Subjects

Eight healthy male volunteers were included in the present study. Exclusion criteria were age <18 y or >40 y, major mental or physical problems, and use of psychopharmaceuticals such as SSRIs or hard drugs such as ecstasy. All volunteers had to complete the Beck Depression Inventory (BDI (*20*)), a validated depression questionnaire, before inclusion to exclude depression. Participants with a BDI score of ≥10 were excluded. Written informed consent was obtained from all subjects, and the study was approved by the local medical ethics committee.

Study Procedure

We used a double-blind, placebo-controlled, crossover design to study the effect of the SSRI paroxetine on binding of ^{123}I-FP-CIT to DATs and SERTs. Therefore, all 8 subjects participated in 2 different sessions with an interval of 1–6 wk between the 2 sessions. Twenty-seven and 3 h before injection with ^{123}I-FP-CIT, the subjects had to take 20 mg (2 tablets of 10 mg) of the SSRI paroxetine (*21*) orally or an equal number of placebo tablets at home. This last time point was chosen because approximately 3 h after oral intake of 20 mg paroxetine, the mean plasma concentration of paroxetine is at its highest level in healthy control subjects (*22*). Both the volunteer and the examiner were unaware of the content of the capsules. Three hours after intake of the last dose of 20 mg paroxetine or placebo, ^{123}I-FP-CIT was injected intravenously as a bolus (approximately 110 MBq). Per session, 2 brain SPECT scans were acquired, at 1 h as well as 3 h after injection. Three hours after injection has been shown to be an optimal time point to assess binding to DAT in the striatum (*23*). The brain SPECT scan 1 h after injection was acquired because Abi-Dargham et al. (*24*) showed that peak specific binding of ^{123}I-FP-CIT in the midbrain occurred approximately at this particular time point, followed by slow washout of activity. Finally, at 2 h after injection of the radiotracer, planar acquisitions of emission scans of the lungs were performed to assess uptake of ^{123}I-FP-CIT in lung tissue, as lungs contain high densities of SERTs (*19*), and at this particular time point lung uptake of ^{123}I-FP-CIT is clearly visible (*25*).

Just before the start of acquisition of the brain SPECT scan 3 h after injection of the radiotracer, venous blood samples were taken for analysis of plasma paroxetine levels.

After 1–6 wk, the procedure was repeated and subjects who were given paroxetine at the first session got placebo at the second session, and vice versa (crossover design).

^{123}I-FP-CIT Brain SPECT and Planar Lung Imaging

Subjects were examined using SPECT and the ligand ^{123}I-FP-CIT, which has a high affinity for the DAT and a somewhat lower affinity for the SERT (*17*). Radiosynthesis of ^{123}I-FP-CIT was performed as described earlier (*25*). The specific activity amounted to ≥185 MBq/nmol, and the radiochemical purity of the solution was >98%. At both sessions approximately 110 MBq (3 mCi) ^{123}I-FP-CIT were injected intravenously as a bolus. Subjects received a potassium iodide solution to block thyroid uptake of free radioactive iodide.

SPECT studies were performed using a 12-detector, single-slice brain-dedicated scanner (Neurofocus, which is an upgrade of the Strichman Medical Equipment 810X system; NeuroPhysics Corp.) with a full width at half-maximum resolution of approximately 6.5 mm, throughout the 20-cm field of view (http://www.neurophysics.com). After positioning of the subjects with the head parallel to the orbitomeatal line, axial slices parallel and upward from the orbitomeatal line to the vertex were acquired in 5-mm steps. Each acquisition consisted of approximately 15 slices with 2.5-min scanning time per slice, acquired in a 64 × 64 matrix. The energy window was set at 135–190 keV.

Lung uptake of ^{123}I-FP-CIT was assessed by using a single-head γ-camera (Diacam or Orbiter; Siemens, dependent on availability). On these systems, a low-energy, all-purpose, parallel-hole collimator was used, and the peak energy was centered at 159 keV with a 15% window. The acquisition time was always 5 min, using a matrix of 256 × 256 pixels. A reference source of approximately 2 MBq ^{123}I was imaged together with the object or directly after the subject was imaged.

Image Reconstruction and Analysis

Attenuation correction of all brain SPECT images was performed as described earlier (*3*). Images were reconstructed in

3-dimensional mode (http://www.neurophysics.com). For quantification, a ROI analysis was performed. Standardized templates of 2-dimensional ROIs were drawn with help of a high-resolution MRI and a brain atlas. ROIs for striatum, midbrain, (hypo)thalamus, occipital cortex, and cerebellum were used, as described earlier (*12*). The ROIs were positioned on the SPECT slices by the same examiner, who was unaware of the content of the pretreatment. For the right and left striatum and the left and right occipital cortex, a template with irregular ROIs, according to the contour of the putamen and caudate nucleus and occipital cortex, was positioned on 4 consecutive axial slices with the highest striatal activity. Individual variation required movement of the fixed ROIs, without changing size and shape, within the template for optimal fitting. As in previous studies (*12*), we defined the inferior level of the (hypo)thalamus to correspond with the inferior level of the striatum. For the (hypo)thalamic area, a template with a round-shaped ROI was placed on 4 SPECT slices with the highest (hypo)thalamic activity. The superior level of the midbrain was defined to coincide with the most superior slice without visible striatal activity. For this midbrain area, a template with a round-shaped ROI was placed on 4 SPECT slices with the highest activity of the midbrain. For the cerebellum, a template with an irregular-shaped ROI was positioned on 3 SPECT slices with the highest cerebellar activity. Mean striatal and mean occipital binding activities were averaged from right and left ROIs. Activity in the cerebellum and occipital cortex was assumed to represent nondisplaceable activity (nonspecific binding and free radioactivity). Finally, specific-to-nonspecific binding ratios were calculated as (activity in ROI minus nonspecific binding/nonspecific binding) (*26*).

Because lung tissue is rich in SERTs (*19*), and previous β-CIT studies suggested that blockage of peripheral SERTs may play a role in the increased striatal binding after the use of SSRIs (*15*), quantification of ^{123}I-FP-CIT uptake in lungs was also performed by a ROI method. ROIs were drawn over left and right lungs (Fig. 1), over the shoulder (representing nonspecific binding; Fig. 1), and over the ^{123}I source, using an emission scan of 1 subject showing clear uptake in the lungs. These ROIs were saved as a template (Fig. 1), and this template was used for all other individual emission images. Consequently, the shapes and sizes (i.e., number of pixels) analyzed were kept constant, which will reduce intra- and interobserver variability. Moreover, the ROIs were relatively large to further minimize variability in the quantification. Finally, the background-corrected lung counts were converted to megabecquerels of activity by application of a calibration factor determined from a known amount of ^{123}I in air (the ^{123}I source). All data were corrected for radioactive decay. For each person and session, decay-corrected data were converted to the percentage of injected activity (%IA) by dividing lung activity by the total amount of injected activity and multiplying by 100.

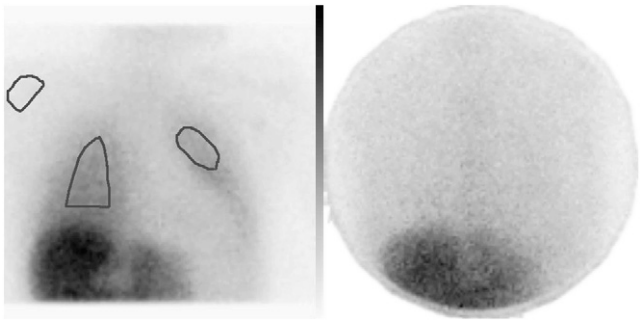

FIGURE 1. Planar scintigraphy of lung uptake of ^{123}I-FP-CIT in healthy young male volunteer, at placebo session (left) and paroxetine session (right). Lung uptake is clearly visible after placebo but not after paroxetine. Activity is encoded from high (black) to low (white). Template with fixed ROIs for lungs and shoulder is shown on the left.

Measurements of Plasma Paroxetine Levels

Blood samples were obtained 6 h after the last drug administration (which is 3 h after injection of the radiotracer). Blood was collected in heparinized tubes, and within 30 min after drawing, samples were centrifuged at 1,100*g* for 5 min, and plasma was stored at −80°C until analysis. The determination of paroxetine in human plasma was performed by the Laboratory for Clinical and Forensic Toxicology and for Drug Analysis (Department of Pharmacy, Groningen University Medical Center, Groningen, The Netherlands). A sensitive, robust, and selective liquid chromatographic–electrospray ionization tandem mass spectrometric method (LC-ESI-MS/MS; Finnigan TSQ Quantum) was used to quantify levels of paroxetine in plasma. The lower limit of detection was 5 μg/L.

Statistical Analysis. Differences in binding ratios and lung uptake between paroxetine and placebo pretreatment were analyzed using a 2-sided Student *t* test for paired samples. The Kolmogorov–Smirnov test was used to analyze whether data were normally distributed. Statistical significance was defined as $P < 0.05$. Statistical analyses were performed using SPSS 11.5 (SPSS, Inc.).

RESULTS

Subjects

The mean age ± SD of the subjects was 22.3 ± 2.8 y (range, 20–28 y). The mean BDI scores ± SD were 0.5 ± 0.9 (range, 0–2). As BDI scores between 0 and 9 are regarded within the normal range, none of the subjects had clinical depression. At the first session, 5 subjects received the placebo and 3 subjects received paroxetine, and at the second session, vice versa.

Analysis of ^{123}I-FP-CIT Binding to Striatal DAT

Data from the ROI analysis were normally distributed. The means and SDs for specific-to-nonspecific striatal ^{123}I-FP-CIT binding ratios are described in Table 1. The mean binding ratios of striatal ^{123}I-FP-CIT were higher after paroxetine intake than after the placebo, at both 1 and 3 h after injection, independent of whether the nonspecific binding was assessed in the cerebellum or in the occipital cortex. Three hours after injection, these ratios were statistically significantly higher after paroxetine intake than after placebo intake in the DAT-rich striatum, when activity in the occipital cortex was used to assess nonspecific binding but not when activity in the cerebellum was used to assess nonspecific binding.

Analysis of ^{123}I-FP-CIT Binding to Central SERTs and to SERTs in Lungs

The paired differences were normally distributed. Figure 2 shows a representative SPECT scan obtained 1 h after injection of ^{123}I-FP-CIT (transversal slices). ^{123}I-FP-CIT binding in the striatum is intense, whereas binding in the midbrain

TABLE 1
Specific-to-Nonspecific ^{123}I-FP-CIT Binding Ratios, Obtained 1 and 3 Hours After Injection of Radiotracer, in a DAT-Rich Brain Area (Striatum) and in SERT-Rich Areas (Midbrain and Diencephalon)

^{123}I-FP-CIT Binding	1 h after injection*		3 h after injection	
	Placebo	Paroxetine†	Placebo	Paroxetine
DAT				
Striatum/cer.‡	2.23 ± 0.67	2.37 ± 0.55	3.99 ± 0.44	4.12 ± 0.90
Striatum/occ.	2.99 ± 0.75	3.15 ± 0.48	4.20 ± 0.37	4.57 ± 0.53§
SERT				
Midbrain/cer.	0.10 ± 0.11	0.01 ± 0.15	0.20 ± 0.20	−0.02 ± 0.08§
Midbrain/occ.	0.36 ± 0.08	0.25 ± 0.15§	0.24 ± 0.16	0.07 ± 0.09§
Diencephalon/cer.	0.23 ± 0.17	0.16 ± 0.17	0.43 ± 0.20	0.26 ± 0.19¶
Diencephalon/occ.	0.53 ± 0.13	0.44 ± 0.18¶	0.48 ± 0.10	0.37 ± 0.12¶

*In 1 control subject, cerebellum and midbrain area were not adequately scanned 1 h after injection of radiotracer; therefore, ratios of specific over cerebellar (cer.) binding are provided for 7 control subjects instead of 8.

†Placebo or paroxetine tablets (20 mg per session) were taken orally approximately 3 and 27 h before injection of radiotracer.

‡Ratios are expressed as specific to nonspecific binding (±SD). Nonspecific binding represents activity in cerebellum (cer.) or occipital cortex (occ.).

§Statistically significantly different from placebo condition.

¶A trend for statistically significant difference ($P = 0.054-0.14$).

Healthy control subjects ($n = 8$) received placebo or paroxetine before injection of radiotracer (double-blind, crossover study design).

area and in the diencephalon was much lower than that in the striatum but higher than uptake in the cerebellum or occipital cortex. The means and SD (SDs) for specific-to-nonspecific ^{123}I-FP-CIT binding ratios to central SERTs are described in Table 1. After paroxetine treatment, binding ratios in the SERT-rich midbrain and diencephalon (hypothalamus/thalamus) were lower than that after placebo treatment—both at 1 and 3 h after injection—reaching significance particularly in the midbrain. Figure 3 shows a representative transversal slice of activity at the level of the midbrain 3 h after injection after placebo pretreatment (Fig. 3 left) and lower uptake after paroxetine pretreatment (Fig. 3 right).

Lung uptake of ^{123}I-FP-CIT was statistically significantly lower after paroxetine intake than after placebo intake. After the placebo, the specific lung uptake was 0.97 ± 0.44 %IA, whereas after paroxetine this uptake was 0.56 ± 0.35 %IA. Figure 1 shows intense lung uptake at the placebo session but almost no uptake during the paroxetine session.

Analysis of Subgroup with Detectable Paroxetine Plasma Levels

In 5 of the 8 participants, plasma paroxetine levels were higher than the detection limit (5 μg/L) at the paroxetine session (range, 15–34 μg/L) but not detectable at the placebo session (i.e., <5 μg/L). In the remaining 3 participants, paroxetine plasma levels were below the detection limit, at both sessions. The data of the subgroup with positive paroxetine levels are presented in Table 2. After analysis of these data, similar conclusions can be drawn as from the analysis of data from the whole study group: ^{123}I-FP-CIT is significantly blocked in SERT-rich brain areas, whereas specific striatal-to-occipital cortex binding ratios were significantly increased after paroxetine (approximately 11%). However, in this particular subgroup of participants, ^{123}I-FP-CIT binding not only is significantly blocked in the SERT-rich midbrain but also in the SERT-rich diencephalon. As in the complete group, in this subgroup uptake in lung tissue is also significantly lower after paroxetine than after placebo (0.59 ± 0.38 %IA and 0.84 ± 0.37 %IA, respectively).

DISCUSSION

The main finding of this study is that ^{123}I-FP-CIT binding ratios in the striatum significantly increased after paroxetine intake. To our knowledge, this study is the first that showed that ^{123}I-FP-CIT labels not only striatal DATs but also SERTs in vivo and that lung uptake of ^{123}I-FP-CIT is associated with binding to SERTs. Because of the unique study design, potential confounders such as age, sex, and depression were excluded, as we included only men within a small age range without depression.

Our study showed that ^{123}I-FP-CIT binding ratios in the striatum were significantly higher after paroxetine than after placebo intake. This finding is in line with findings from recent studies using ^{123}I-β-CIT SPECT (*12–14*). Interestingly, the specific striatal-to-occipital ^{123}I-FP-CIT binding ratios were significantly increased by approximately 10% but no significant increase was observed when cerebellar uptake was used to evaluate nonspecific binding. This observation is very relevant, as occipital binding is most frequently used to assess nonspecific binding in ^{123}I-FP-CIT SPECT studies (*3–7,10,11*). Such an approach to analyze scans may thus lead to an overestimation of the striatal binding ratios in patients on SSRIs. It is of interest that the presently observed increase is less pronounced than that in previous studies using ^{123}I-β-CIT as a radiotracer (*12,13*).

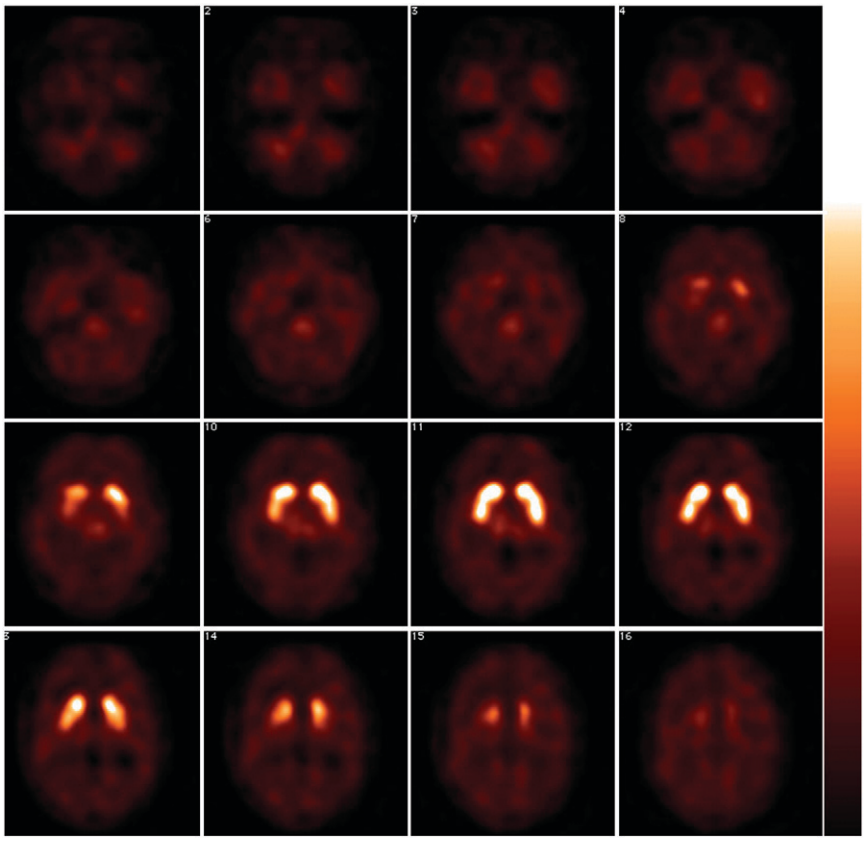

FIGURE 2. Transversal slices of ^{123}I-FP-CIT SPECT scan, obtained in healthy young male volunteer 1 h after injection of radiotracer (placebo pretreatment). Intense and symmetric uptake is visualized in striatum. Binding is also visualized in midbrain and diencephalon area, which is higher than activity in cerebellum and cortical areas but much lower than binding in striatum. Activity is color encoded from high (white) to low (black).

This finding is in line with the observation that ^{123}I-FP-CIT is more selective than ^{123}I-β-CIT for the DAT (*17*). Indeed, although Figure 1 shows that uptake in SERT-rich areas is higher than background activity, the ratios in SERT-rich brain areas are very low compared with these ratios in the DAT-rich striatum.

Our present observation that paroxetine influences only specific striatal-to-occipital ^{123}I-FP-CIT binding ratios, but not striatal to cerebellar ratios, is in line with the observation that SERT expression is higher in cortical areas than that in the cerebellum, although in both areas the expression is extremely low (*21*). In addition, studies performed on rats have shown that ^{123}I-FP-CIT binding in the occipital cortex, but not in the cerebellum, could be displaced by an SSRI (*2*). Interestingly, previous studies showed that striatal binding ratios increased significantly after the use of an SSRI when ^{123}I-β-CIT was used as a radioligand and the cerebellum was used as a reference region (*12–15*). Although the expression of SERTs is very low in the cerebellum, it is not negligible (*21*). In addition, the affinity of β-CIT for the SERT is higher than that of FP-CIT. This different property of both tracers might be the reason that in the present study the striatal-to-cerebellar ^{123}I-FP-CIT binding ratio was not significantly increased after paroxetine. However, this finding does not exclude the observation that when the cerebellum is used as a reference region an effect on the striatal-to-cerebellar ratio does exist after the use of an SSRI and that such an effect might be detected in future studies in larger cohorts. Nonetheless, when taking into account our present findings, it is likely that if such an effect exits, it will be small.

In the present study we did not resolve the cause of the observed increased striatal ^{123}I-FP-CIT ratio after the use of

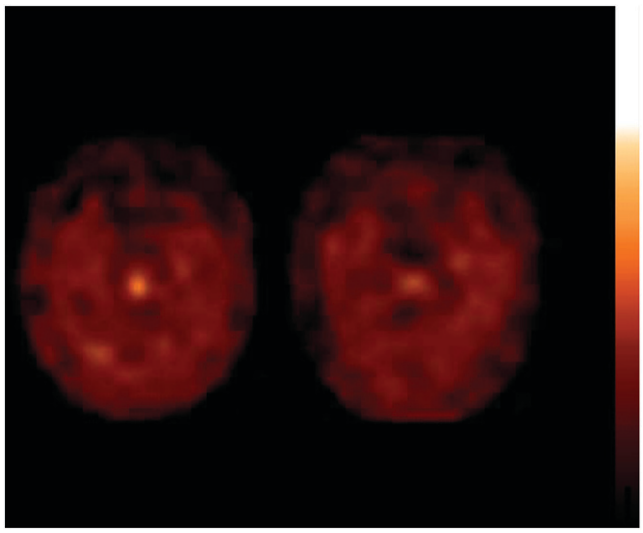

FIGURE 3. Transversal slices of ^{123}I-FP-CIT SPECT scan at level of temporal cortex and midbrain, obtained in healthy young male volunteer 3 h after injection of radiotracer. After placebo pretreatment there is clear visualization of activity in midbrain (left), which is much lower after paroxetine pretreatment (right). Activity is color encoded from high (white) to low (black).

TABLE 2
Specific-to-Nonspecific ^{123}I-FP-CIT Binding Ratios, Obtained 1 and 3 Hours After Injection of Radiotracer, in DAT-Rich Brain Area (Striatum) and in SERT-Rich Areas (Midbrain and Diencephalon)

^{123}I-FP-CIT Binding	1 h after injection		3 h after injection	
	Placebo	Paroxetine*	Placebo	Paroxetine
DAT				
Striatum/cer.†	2.30 ± 0.80	2.10 ± 0.27	3.95 ± 0.36	3.71 ± 0.55
Striatum/occ.	2.95 ± 0.97	2.93 ± 0.44	3.97 ± 0.15	4.41 ± 0.43‡
SERT				
Midbrain/cer.	0.13 ± 0.12	−0.04 ± 0.14‡	0.21 ± 0.14	−0.04 ± 0.05‡
Midbrain/occ.	0.35 ± 0.10	0.22 ± 0.17‡	0.21 ± 0.12	0.10 ± 0.06
Diencephalon/cer.	0.29 ± 0.16	0.08 ± 0.13§	0.51 ± 0.17	0.17 ± 0.15‡
Diencephalon/occ.	0.54 ± 0.15	0.38 ± 0.20§	0.51 ± 0.10	0.34 ± 0.13‡

*Placebo or paroxetine tablets (20 mg per session) were taken orally approximately 3 and 27 h before injection of radiotracer.

†Ratios are expressed as specific to nonspecific binding (±SD). Nonspecific binding represents activity in cerebellum (cer.) or occipital cortex (occ.).

‡Statistically significantly different from placebo condition.

§A trend for statistically significant difference ($P = 0.07-0.09$).

Healthy control subjects ($n = 5$) received placebo or paroxetine before injection of radiotracer (double-blind, crossover study design). In these 5 control subjects, at the paroxetine session, paroxetine plasma levels were >5 μg/L, whereas at the placebo session, paroxetine was not detectable in plasma (<5 μg/L).

paroxetine, but it may be of interest to speculate on the mechanism by which an SSRI induces a significant increase in the striatal ^{123}I-FP-CIT ratio. Although we could not exclude the fact that the increase in striatal ^{123}I-FP-CIT binding ratios after paroxetine represents a direct interaction between the dopaminergic and serotonergic system (*13*), another explanation for this phenomenon might be as follows: Paroxetine blocks the low, but specific, binding of ^{123}I-FP-CIT to SERTs in the occipital cortex, which induces an increase in the striatal binding ratio. Mathematically, particularly changes in the denominator will have a large impact on the calculation of a ratio. On the other hand, the extremely low expression of cerebellar SERT, in combination with a modest affinity of ^{123}I-FP-CIT for SERTS, may prevent the ability of paroxetine to influence specific striatal-to-cerebellar ^{123}I-FP-CIT binding ratios. Against our postulate one may argue that the SERT density is higher in striatum than that in occipital cortex and that blockage of SERTs thus might lead theoretically to a lower striatal-to-occipital cortex ratio. However, in this ratio, the numerator is dominated by binding of ^{123}I-FP-CIT to DATs. SERT blockage may indeed induce a lower absolute striatal ^{123}I-FP-CIT binding, and this absolute change in binding may be even larger than the absolute change of ^{123}I-FP-CIT binding in the occipital cortex, but the percentage change due to this blockage is larger in the denominator than that in the numerator. Although our present data show a significant increase in striatal ^{123}I-FP-CIT binding ratios, it is unlikely that this relative small effect of approximately 10% increase will affect visual assessments of ^{123}I-FP-CIT SPECT images.

To our knowledge, this is the first study that validated the use of ^{123}I-FP-CIT SPECT to assess SERTs in vivo in the human brain using a double-blind, placebo-controlled study in which the same healthy volunteers were examined with and without pretreatment with an SSRI. Our finding is in line with in vitro data which showed that FP-CIT has a moderate affinity for SERTs (*17*). In addition, and in agreement with previous ^{123}I-β-CIT SPECT studies (*12*), uptake in the midbrain was blocked with an SSRI to a greater extent than uptake in the hypothalamus/thalamus. It has been shown, however, that ^{123}I-β-CIT binding in the human thalamus was associated primarily with binding to norepinephrine transporters, instead of SERTs (*27*). However, on the basis of in vitro data, which showed that the affinity of FP-CIT is low for the norepinephrine transporter (IC_{50}, 140 nmol/L (*17*)), it is unlikely that in vivo ^{123}I-FP-CIT binding in the diencephalon represents primarily binding to norepinephrine transporter. Nonetheless, one has to take into account the observation that the affinity has been measured in striatal rat tissue. Therefore, differences in affinity of FP-CIT between species could not be excluded. More studies are needed to test whether ^{123}I-FP-CIT binds in vivo to norepinephrine transporters.

Although our finding that ^{123}I-FP-CIT labels SERTs in vivo is novel and challenging, it is not an attractive radioligand to evaluate the expression of this transporter in vivo, because the specific binding ratios are rather low, and other SPECT tracers (e.g., ^{123}I-β-CIT) have a higher affinity for SERTs, resulting in higher uptake ratios. Moreover, recently selective SERT radiotracers have been developed successfully, for both PET and SPECT (*28,29*).

This study shows that ^{123}I-FP-CIT uptake in lungs is associated with binding to SERTs. Previous β-CIT and PET studies, using selective radiotracers for the SERT, suggested that blockage of radioligand binding to peripheral SERTs

may influence quantification due to an increased availability of brain activity (*12,15,30*). Indeed, in a previous ^{123}I-β-CIT SPECT study, we found increased total radioactivity in the cerebellum after the use of an SSRI (*12*). However, in the present study, we did not observe such a phenomenon (data not shown). Recent studies on the role of SERTs in lung tissue have supported a central role of SERTs in the pathogenesis of idiopathic pulmonary hypertension (*31*). Nevertheless, further studies are needed to replicate our preliminary finding of detectable SERT binding in lungs with ^{123}I-FP-CIT.

Cocaine *N*-demethylation by microsomal cytochrome P-450 (CYP) is the principal pathway in cocaine bioactivation and hepatoxicity (*32*). Because ^{123}I-FP-CIT is a cocaine derivative, *N*-demethylation of FP-CIT will also take place in humans, and after *N*-demethylation an ^{123}I-labeled metabolite, nor-β-CIT, is formed (*33*), although in very small amounts (*34*). CYP3A plays a major role in the *N*-demethylation of cocaine (*31,35*) and, consequently, presumably also in the *N*-demethylation of ^{123}I-FP-CIT. Because paroxetine is a substrate and a blocker for CYP2D6, but not for CYP3A, it is unlikely that paroxetine has influenced the *N*-demethylation of ^{123}I-FP-CIT in this study.

In this study, paroxetine has been used as a SERT blocker. Although we have no direct evidence that other SSRIs will have the same effects on striatal FP-CIT binding ratios, it is likely that this will be true. Yet, within the groups of SSRIs, 1 SSRI has a relatively high affinity for the DAT—that is, sertraline (affinity for DAT, approximately 20 nmol/L (*36*)). It may be hypothesized that the DAT blocking effects of sertraline on striatal ^{123}I-FP-CIT binding ratio are counterbalanced by its SERT blocking effects, although this has to been proven in future studies.

A limitation of the present study was that intake of paroxetine or placebo tablets was not supervised and that in 3 participants paroxetine was not detectable in plasma. Therefore, it may be possible that these 3 participants did not take all of their tablets at home. However, from the undetectable paroxetine plasma levels we cannot conclude that these 3 participants did not take their tablets. A recent article on the pharmacokinetics of paroxetine showed that after 1 dose of 20 mg of paroxetine, plasma levels were highly variable between subjects, which is in line with our present findings, and that in 4 of the 9 subjects, plasma levels were lower than 5 μg/L 5 h after oral intake of the tablet (*22*). On the basis of this information, we assumed that a single dose of 20 mg paroxetine might not induce high enough plasma concentrations to be detectable in all participants. Because paroxetine is not only an inhibitor for the liver microsomal CYP2D6 system but also a substrate, we postulated that 2 doses of 20 mg would induce plasma paroxetine levels high enough to be detectable with the LC-ESI-MS/MS system. Nonetheless, despite the elevated dose, we found that in 3 of the 8 participants plasma levels were lower than 5 μg/L at 6 h after intake of the last dose. However, it is possible that if we had the availability of a technique with lower detection limits (*22*) we might have been able to detect paroxetine in plasma of all our participants. Moreover, another study showed that although paroxetine intake was monitored for 8 consecutive days, in 1 case no paroxetine levels were detectable, presumably because of a fast metabolism of the drug (this subject was found to carry at least 3 functional CYP2D6 genes (*37*)). Finally, Meyer et al. (*38*) found that the plasma concentration of paroxetine needed to obtain 50% SERT occupancy in the striatum is only 2.7 μg/L. All in all, we did not exclude these 3 subjects, because it is still conceivable that they took their tablets and because ^{123}I-FP-CIT uptake in lung tissue was lower (although not statistically significant) at the paroxetine session than at the placebo session in all 3 participants (data not shown). For example, Figure 3 represents ^{123}I-FP-CIT uptake in lung tissue from one of the participants with undetectable paroxetine levels in his blood samples at both sessions, whereas the images clearly show blockage of lung uptake at the paroxetine session compared with the placebo session. On the other hand, ^{123}I-FP-CIT binding was not always lower in SERT-rich brain areas, at all studied time points, whereas this was true for the subgroup with detectable paroxetine in their blood (data not shown). Nevertheless, we also presented separately the data for the 5 participants who had detectable paroxetine levels in their blood at the paroxetine session. It is important to note that all findings in the whole group under study (n = 8) could be reproduced in the subgroup of participants with positive paroxetine samples; therefore, we consider all conclusions from the study related to the effects of paroxetine on ^{123}I-FP-CIT binding to be sound.

CONCLUSION

In this placebo-controlled, double-blind, crossover study, we show that the SSRI paroxetine induces a significant increase in specific striatal-to-occipital ^{123}I-FP-CIT binding ratios in healthy control subjects. In addition, paroxetine was able to block ^{123}I-FP-CIT binding ratios in SERT-rich brain area and in lungs. Therefore, for the quantification of ^{123}I-FP-CIT SPECT studies, the effects of paroxetine, and presumably also other SSRIs, should be considered.

ACKNOWLEDGMENTS

The authors acknowledge Eric Ruhe and Arno Vyth for providing the placebo and paroxetine tablets. Yuma Bijleveld and Rob Kuiper are gratefully acknowledged for their help in the logistics concerning the analysis of the paroxetine plasma levels. The Department of Pharmacy at the Groningen University Medical Center is acknowledged for the assessment of the paroxetine plasma concentrations. Finally, GE Healthcare Eindhoven is gratefully acknowledged for their generous gift of the radiotracer.

REFERENCES

1. Nirenberg MJ, Chan J, Vaughan RA, Uhl GR, Kuhar MJ, Pickel VM. Immunogold localization of the dopamine transporter: an ultrastructural study of the rat ventral tegmental area. *J Neurosci.* 1997;17:4037–4044.
2. Booij J, Andringa G, Rijks LJM, et al. [^{123}I]FP-CIT binds to the dopamine transporter as assessed by biodistribution studies in rats and SPECT studies in MPTP-lesioned monkeys. *Synapse.* 1997;27:183–190.
3. Booij J, Tissingh G, Boer GJ, et al. [^{123}I]SPECT shows a pronounced decline of striatal labelling in early and advanced Parkinson's disease. *J Neurol Neurosurg Psychiatry.* 1997;62:133–140.
4. Ishikawa T, Dhawan V, Kazumata K, et al. Comparative nigrostriatal dopaminergic imaging with iodine-123-beta-CIT-FP/SPECT and fluorine-18-FDOPA/PET. *J Nucl Med.* 1996;37:1760–1765.
5. Tissingh G, Booij J, Bergmans P, et al. Iodine-123-N-ω-fluoropropyl-2-β-carbomethoxy-3β-(4-iodophenyl)tropane SPECT in healthy controls and early stage, drug-naive Parkinson's disease. *J Nucl Med.* 1998;39:1143–1148.
6. O'Brien JT, Colloby S, Fenwick J, et al. Dopamine transporter loss visualized with FP-CIT SPECT in the differential diagnosis of dementia with Lewy bodies. *Arch Neurol.* 2004;61:919–925.
7. Stiasny-Kolster K, Doerr Y, Möller JC, et al. Combination of 'idiopathic' REM sleep behaviour disorder and olfactory dysfunction as possible indicator for alpha-synucleinopathy demonstrated by dopamine transporter FP-CIT-SPECT. *Brain.* 2005;128:126–137.
8. Van Laere K, Casteels C, De Ceuninck L, et al. Dual-tracer dopamine transporter and perfusion SPECT in differential diagnosis of parkinsonism using template-based discriminant analysis. *J Nucl Med.* 2006;47:384–392.
9. Benamer HTS, Patterson J, Grosset DG, et al. Accurate differentiation of parkinsonism and essential tremor using visual assessment of [^{123}I]-FP-CIT SPECT imaging: the [^{123}I]-FP-CIT study group. *Mov Disord.* 2000;15:503–510.
10. Lorberboym M, Treves TA, Melamed E, Lampl Y, Hellmann M, Djaldetti R. [^{123}I]-FP/CIT SPECT imaging for distinguishing drug-induced parkinsonism from Parkinson's disease. *Mov Disord.* 2006;21:510–514.
11. Booij J, Speelman JD, Horstink MWIM, Wolters EC. The clinical benefit of imaging striatal dopamine transporters with [^{123}I]FP-CIT SPET in differentiating patients with presynaptic parkinsonism from those with other forms of parkinsonism. *Eur J Nucl Med.* 2001;28:266–272.
12. de Win MML, Habraken JBA, Reneman L, van den Brink W, den Heeten GJ, Booij J. Validation of [^{123}I]β-CIT SPECT to assess serotonin transporters in vivo in humans: a double-blind, placebo-controlled, crossover SPECT study with the selective serotonin reuptake inhibitor citalopram. *Neuropsychopharmacology.* 2005;30:996–1005.
13. Kugaya A, Seneca NM, Snyder PJ, et al. Changes in human in vivo serotonin and dopamine transporter availabilities during chronic antidepressant administration. *Neuropsychopharmacology.* 2003;28:413–420.
14. Tauscher J, Pirker W, de Zwaan M, Asenbaum S, Brücke T, Kasper S. *In vivo* visualization of serotonin transporters in the human brain during fluoxetine treatment. *Eur Neuropsychopharmacol.* 1999;9:177–179.
15. Scheffel U, Kim S, Cline EJ, Kuhar MJ. Occupancy of the serotonin transporter by fluoxetine, paroxetine, and sertraline: in vivo studies with [^{125}I]RTI-55. *Synapse.* 1994;16:263–268.
16. Neumeyer JL, Wang S, Gao Y, et al. N-ω-fluoroalkyl analogs of (1R)-2β-carbomethoxy-3β-(4-iodophenyl)-tropane (β-CIT): radiotracers for positron emission tomography and single photon emission computed tomography imaging of dopamine transporters. *J Med Chem.* 1994;37:1558–1561.
17. Scheffel U, Lever JR, Abraham P, et al. N-substituted phenyltropanes as in vivo binding ligands for rapid imaging studies of the dopamine transporter. *Synapse.* 1997;25:345–349.
18. Slaughter JR, Parker JC, Martens MP, Smarr KL, Hewett JE. Prevalence, clinical manifestations, etiology, and treatment of depression in Parkinson's disease. *J Neuropsychiatry Clin Neurosci.* 2001;13:187–196.
19. Suhara T, Sudo Y, Yoshida K, et al. Lung as reservoir for antidepressants in pharmacokinetic drug interactions. *Lancet.* 1998;351:332–335.
20. Beck AT, Ward CH, Mendelson M, Mock J, Erbaugh J. An inventory for measuring depression. *Arch Gen Psychiatry.* 1961;4:561–571.
21. Bäckström I, Bergström M, Marcusson J. High affinity [^{3}H]paroxetine binding to serotonin uptake sites in human brain tissue. *Brain Res.* 1989;486:261–268.
22. Segura M, Ortuno J, Farre M, et al. Quantitative determination of paroxetine and its 4-hydroxy-3-methoxy metabolite in plasma by high-performance liquid chromatography/electrospray ion trap mass spectrometry: application to pharmacokinetic studies. *Rapid Commun Mass Spectrom.* 2003;17:1455–1461.
23. Booij J, Hemelaar JTGM, Speelman JD, de Bruin K, Janssen AGM, van Royen EA. One-day protocol for imaging of the nigrostriatal pathway in Parkinson's disease by [^{123}I]FPCIT SPECT. *J Nucl Med.* 1999;40:753–761.
24. Abi-Dargham A, Gandelman MS, DeErausquin GA, et al. SPECT imaging of dopamine transporters in human brain with iodine-123-fluoroalkyl analogs of β-CIT. *J Nucl Med.* 1996;37:1129–1133.
25. Booij J, Busemann Sokole E, Stabin MG, Janssen AGM, de Bruin K, van Royen EA. Human biodistribution and dosimetry of [^{123}I]FP-CIT: a potent radioligand for imaging of dopamine transporters. *Eur J Nucl Med.* 1998;25:24–30.
26. Laruelle M, Wallace E, Seibyl JP, et al. Graphical, kinetic, and equilibrium analyses of in vivo [^{123}I]β-CIT binding to dopamine transporters in healthy human subjects. *J Cereb Blood Flow Metab.* 1994;14:982–994.
27. Farde L, Halldin C, Müller L, Suhara T, Karlsson P, Hall H. PET study of [^{11}C]β-CIT binding to monoamine transporters in the monkey and human brain. *Synapse.* 1994;2:93–103.
28. Huang Y, Hwang DR, Narendran R, et al. Comparative evaluation in nonhuman primates of five PET radiotracers for imaging the serotonin transporters: [^{11}C]McN 5652, [^{11}C]ADAM, [^{11}C]DASB, [^{11}C]DAPA, and [^{11}C]AFM. *J Cereb Blood Flow Metab.* 2002;22:1377–1398.
29. Choi SR, Hou C, Oya S, et al. Selective in vitro and in vivo binding of [^{125}I]ADAM to serotonin transporters in rat brain. *Synapse.* 2000;38:403–412.
30. Szabo Z, McCann UD, Wilson AA, et al. Comparison of (+)-^{11}C-McN5652 and ^{11}C-DASB as serotonin transporter radioligands under various experimental conditions. *J Nucl Med.* 2002;43:678–692.
31. Guignabert C, Izikki M, Tu LI, et al. Transgenic mice overexpressing the 5-hydroxytryptamine transporter gene in smooth muscle develop pulmonary hypertension. *Circ Res.* 2006;98:1323–1330.
32. Arinc E, Bozcaarmutlu A. Catalyzation of cocaine N-demethylation by cytochromes P4502B, P4503A, and P4502D in fish liver. *J Biochem Mol Toxicol.* 2003;17:169–176.
33. Boja JW, Kuhar MJ, Kopajtic T, et al. Secondary amine analogues of 3 beta-(4′-substituted phenyl)tropane-2 beta-carboxylic acid esters and N-norcocaine exhibit enhanced affinity for serotonin and norepinephrine transporters. *J Med Chem.* 1994;37:1220–1223.
34. Bergström K, Halldin C, Lundkvist C, et al. Characterization of C-11 or I-123 β-CIT-FP ad β-CIT-FE metabolism measured in monkey and human plasma: identification of two labelled metabolites with HPLC. *Hum Psychopharmacol.* 1996;11:483–490.
35. Pellinen P, Honkakoski P, Stenback F. Cocaine N-demethylation and the metabolism-related hepatotoxicity can be prevented by cytochrome P450 3A inhibitors. *Eur J Pharmacol.* 1994;270:35–43.
36. Owens MJ, Knight DL, Nemeroff CB. Second-generation SSRIs: human monoamine transporter binding profile of escitalopram and R-fluoxetine. *Biol Psychiatry.* 2001;50:345–350.
37. Lam YW, Gaedigk A, Ereshefsky L, Alfaro CL, Simpson J. CYP2D6 inhibition by selective serotonin reuptake inhibitors: analysis of achievable steady-state plasma concentrations and the effect of ultrarapid metabolism at CYP2D6. *Pharmacotherapy.* 2002;22:1001–1006.
38. Meyer JH, Wilson AA, Sagrati S, et al. Serotonin transporter occupancy of five selective serotonin reuptake inhibitors at different doses: an [^{11}C]DASB positron emission tomography study. *Am J Psychiatry.* 2004;161:826–835.